

pubs.acs.org/NanoLett Letter

Mechanical Properties and Photomechanical Fatigue of Macro- and Nanodimensional Diarylethene Molecular Crystals

Thiranjeewa I. Lansakara, Fei Tong, Christopher J. Bardeen,* and Alexei V. Tivanski*



Cite This: Nano Lett. 2020, 20, 6744-6749



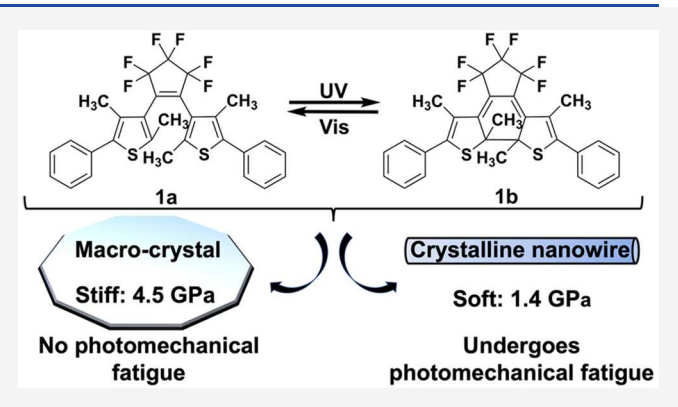
ACCESS

Metrics & More

Article Recommendations

Supporting Information

ABSTRACT: The diarylethene derivative, 1,2-bis(2,4-dimethyl-5-phenyl-3-thienyl)perfluorocyclopentene, undergoes a reversible photoisomerization between its ring-open and ring-closed forms in the solid-state and has applications as a photomechanical material. Mechanical properties of macrocrystals, nanowire single crystals, and amorphous films as a function of multiple sequential UV and visible light exposures have been quantified using atomic force microscopy nanoindentation. The isomerization reaction has no effect on the elastic modulus of each solid. But going from the macro- to the nanowire crystal results in a remarkable over 3-fold decrease in the elastic modulus. The macrocrystal and amorphous solids are highly resistant to photomechanical fatigue, while nanowire crystals show clear evidence of photomechanical fatigue



attributed to a transition from crystal to amorphous forms. This study provides first experimental evidence of size-dependent photomechanical fatigue in photoreactive molecular crystalline solids and suggests crystal morphology and size must be considered for future photomechanical applications.

KEYWORDS: AFM nanoindentation, photomechanical fatigue, photoreversible, molecular crystals, nanowires, Young's modulus

■ INTRODUCTION

Photochemical reactions that occur in the solid crystalline state can be utilized for direct conversion of light energy to macroscopic anisotropic movements of the solid. ^{1,2} The strain built up between the reactant and product crystal phases results in a variety of exciting macroscopic mechanical shape behaviors including bending, ³ twisting, ⁴ expansion, ⁵ contraction, ⁶ fragmentation, ⁷ and coiling. ⁸ Recently, several examples of photochemical reactions that led to mechanical motions of solids were reported, including E-Z photoisomerization, ^{9,10} [2 + 2] ¹¹ and [4 + 4] ^{5,12} photodimerization, linkage isomerization, ¹³ and ring opening—closing isomerization. ^{14–16} Development of photomechanical molecular crystals may enable the creation of actuators that allow facile conversion of light energy into mechanical work.

Diarylethenes are a class of photochromic molecules that undergo a reversible ring opening—ring closing photoisomerization as a result of exposure to visible and ultraviolet (UV) light (Scheme 1). Both isomers are thermally stable with relatively fast conversion times, and the solids show high resistance to photomechanical fatigue. In order to reduce the probability of fracture during photoreaction, nanoscale crystals and composites are often used. For example, 1,2-bis(2,4-dimethyl-5-phenyl-3-thienyl) perfluorocyclopentene (DAE) crystalline nanowires with ~200 nm diameter have been utilized to generate reversible photomechanical motion.

Scheme 1. Photochemical Interconversion between Ring-Open (1a) and Ring-Closed (1b) Isomers with UV (\sim 360 nm) and Visible (\sim 530 nm) Light Exposures

Furthermore, a macroscopic actuator based on DAE derivative nanowires embedded into a template was utilized to reversibly lift an object approximately 10⁴ times its own weight.²⁵ However, beyond 50 cycles evidence of photomechanical fatigue appeared, which was tentatively attributed to molecular interactions between the template walls and DAE nanowires. In contrast, bulk macrocrystals and solutions of DAE showed high stability after more than 500 cycles.

Received: June 25, 2020 Revised: August 20, 2020 Published: August 21, 2020





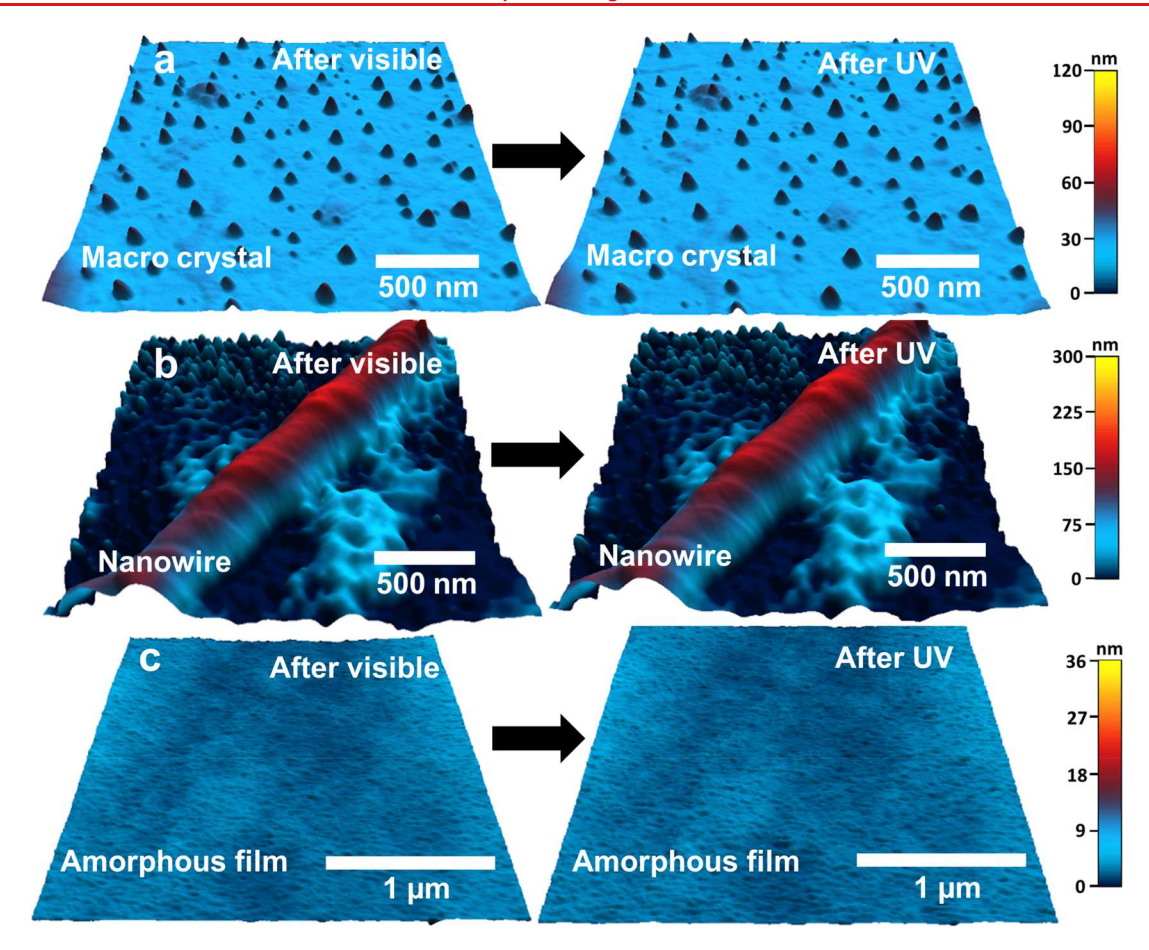


Figure 1. Representative AFM 3D height images of DAE (a) macrocrystal, (b) nanowire single crystal, and (c) amorphous film after visible (left) and UV (right) light exposure. No change in the localized sample topography for each solid was observed as a result of one cycle with visible and UV light exposures.

Photomechanical fatigue is a common issue that hinders the development of materials based on organic photochromism, including photomechanical actuators and optical memories. 12,26 It is generally attributed to a combination of chemical side reactions and irreversible structural changes in the solid such as defect accumulation and fracture.^{27°} But the DAE results suggest that there is a large difference in the fatigue resistance of nanowires versus macrocrystals. While the effect of nanosizing on the electrical properties of semiconductors is reasonably well understood, how morphology at the nanoscale affects mechanical properties of crystalline solids is poorly understood, especially for organic materials²⁸⁻³¹ that are typically softer than inorganic solids.³² Although photomechanical motion and photomechanical fatigue are largely governed by the elastic properties of photomechanical molecular solids,²⁷ studies of the mechanical properties of such solids are scarce.³³

Herein, we elucidate the origin of the photomechanical fatigue observed in the DAE crystalline nanowires. Atomic force microscopy (AFM) nanoindentation is used to measure the elastic modulus (Young's modulus) of solid DAE samples with different morphologies: individual macrocrystals, nanowire single crystals, and amorphous films. These samples are interconverted between the ring-open (1a) and ring-closed (1b) forms using alternating UV and visible light exposures. We demonstrate that the mechanical properties of the two isomers are similar yet vary depending on the crystal morphology and size. Evidence of the photomechanical fatigue

is observed by quantifying a decrease in the Young's modulus of an individual nanowire as a result of repeated UV and visible light exposures. The origin of the photomechanical fatigue is attributed to a transition from crystal to amorphous form in the nanowires.

■ RESULTS AND DISCUSSION

Figure 1 shows representative AFM 3D height images of each DAE sample after visible (~530 nm) and then UV (~360 nm) light exposure. The solid samples underwent a clear change in color from colorless ring-open isomer 1a to blue-colored ringclosed isomer 1b after UV exposure and then back to colorless 1a isomer after visible light exposure. The macrocrystal surface was reasonably flat with 15-30 nm tall rounded features spread across the crystal surface, as also observed for other molecular macrocrystals. 28,34 The nanowires were 2–4 μm long and 180 ± 20 nm in diameter, lying flat on the anodic aluminum oxide (AAO) template surface with features ranging in 20-80 nm in height (Figure 1b). The amorphous film was significantly smoother (Figure 1c) compared to both macrocrystal and nanowire samples. None of the solids exhibited a change in localized AFM-determined sample topography as a result of photoirradiation (root-mean-square roughness for each solid before and after light exposure is reported in Table S1). This is consistent with the relatively small change in molecular geometry upon isomerization with only ~10% expected shortening of the distance between 5- and 5' carbons in the two thiophene rings. 17 Large-scale mechanical motion of

the nanowires (e.g., bending) was prevented by adhesion to the dry AAO template surface.

AFM nanoindentation measurements were carried out after first exposing each solid to visible light to ensure the DAE was initially in the 1a isomer. Representative force versus indentation distance curves are shown in Figure 2a. Young's

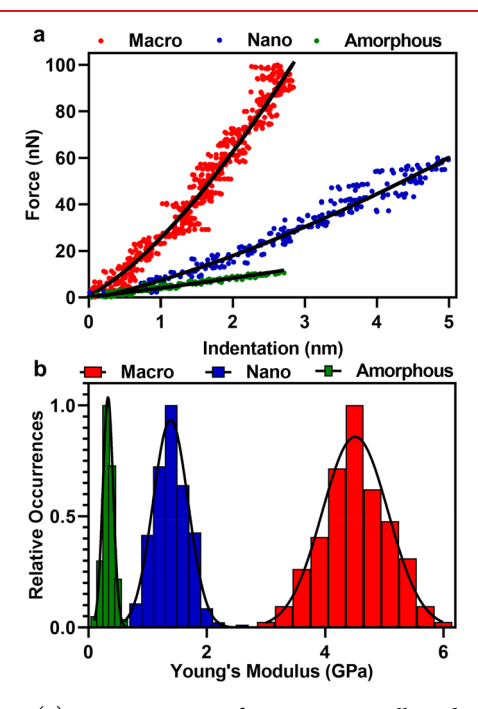


Figure 2. (a) Representative force curves collected on DAE macrocrystal (red), nanowire (blue), and amorphous film (green). Solid black lines are the JKR fit. (b) Histograms of Young's moduli for the DAE macro (red), nanowire (blue), and amorphous film (green). Solid black lines are Gaussian fits.

modulus values were determined by fitting the approach force data to the Johnson-Kendall-Roberts (JKR) elastic contact model. Averaged Young's moduli for each solid at different sample positions were within one standard deviation of each other, enabling us to combine the values from all sample positions for each solid to a single histogram (Figure 2b). The resultant histogram for each sample was fit using a Gaussian function to determine the most probable Young's modulus and corresponding standard deviation.

The most probable Young's moduli for 1a single macrocrystal, nanowire single crystal, and amorphous film were 4.4 \pm 0.4, 1.4 \pm 0.1, and 0.34 \pm 0.04 GPa, respectively. After the samples were exposed to UV light to yield 1b isomer, the macrocrystal undergoes photoinduced movement which was absent for the substrate-deposited nanowire and amorphous film. The AFM nanoindentation measurements before and after light exposure were performed on the macrocrystal over a similar 5 μ m \times 5 μ m sample region which was located using AFM imaging and a top-view optical camera. AFM nanoindentation measurements were performed on similar sample positions for the DAE nanowire and amorphous film samples. The most probable Young's moduli for 1b single macrocrystal, nanowire single crystal, and amorphous film were 4.5 \pm 0.5, 1.3 \pm 0.15, and 0.35 \pm 0.03 GPa, respectively. Since the most probable Young's moduli for the two isomers for each sample were statistically similar, the Young's moduli values for the ring-open and ring-closed isomers were combined into a single

histogram for each sample. Figure 2b displays the combined Young's moduli histogram of single macrocrystal (red), nanowire single crystal (blue), and amorphous film (green) with the Gaussian fits (black). We note that the similar elastic moduli for the two isomers and absence of localized sample topography changes is consistent with the relatively small change in molecular geometry upon isomerization. Irie and coworkers previously showed that the DAE macrocrystals undergo single-crystal to single-crystal photoisomerization with each cycle of the UV and visible light exposure.³⁵ The degree of DAE 1a to 1b conversion efficiency is dependent on the photostationary state and solid sample thickness as a result of a positive photochrome formation. 36,37 For amorphous film and macrocrystal solids, the expected conversion efficiencies from 1a to 1b are 5-10%, similar to 6% conversion observed for a 50 µm thick DAE sample.²⁵ For individual nanowires with thicknesses less than 200 nm, the expected conversion efficiency will likely be closer to 79% observed for the DAE molecules in a hexane solution.³⁸

The Young's modulus of the DAE amorphous film (0.35 GPa) is comparable to low-density polyethylene (0.20–0.30 GPa).³⁹ The Young's modulus of DAE single macrocrystal (4.5 GPa) is in line with values observed for other molecular crystalline solids.^{28,40,41} Surprisingly, the Young's modulus of the DAE nanowire crystal (1.4 GPa) shows a remarkable over 3-fold reduction compared to the macrocrystal. Previous studies have also reported differences in the Young's modulus between macro- and nanodimensional solids.^{28,29,40,42} While the exact origin of the size-dependent mechanical response is unknown, it likely originates from a combination of factors including morphological differences, a decrease in the number of repeat units, and the increasing contribution of surface effects (e.g., surface defects, surface energy effects) as the surface-to-volume ratio increases at the nanoscale.^{28,42–44}

Next, the macrocrystal, nanowire, and amorphous film were repeatedly irradiated with cycles of visible and UV light exposures up to a total of 50 cycles. For each solid, Young's modulus was measured after every 3 cycles until the 15th cycle and every 10 cycles after the 20th cycle. Figure 3 shows the change in the Young's modulus as a function of light exposure cycles for each solid. The Young's modulus of the macrocrystal does not change over 50 light exposure cycles. This is consistent with previous reports that DAE macrocrystals can undergo hundreds of repeated cycles of photo-induced bending without evidence of photomechanical fatigue. The Young's modulus of DAE amorphous film also does not change over 50 cycles of light exposures.

Notably, individual DAE nanowires showed a rapid decrease in the Young's modulus from 1.4 to 1.0 GPa between the 12th and 15th cycle (Figure 3). After 20 cycles, the Young's modulus of the DAE nanowire (0.34 GPa) converges to that of the amorphous film (0.35 GPa). No further changes in the modulus were observed after up to 50 cycles. The decrease of the Young's modulus was uniform across the nanowire. The change in the nanowire elastic modulus is accompanied by the appearance of hysteresis between the approach and retract force data (Figure 4a), which is similar to that observed for the amorphous film (see SI) and indicative of an increasing contribution of viscoelastic effects. The decrease in Young's modulus and appearance of the hysteresis are clear signatures of photomechanical fatigue.

The transition in Young's modulus values for the DAE nanowires due to photomechanical fatigue can be seen clearly

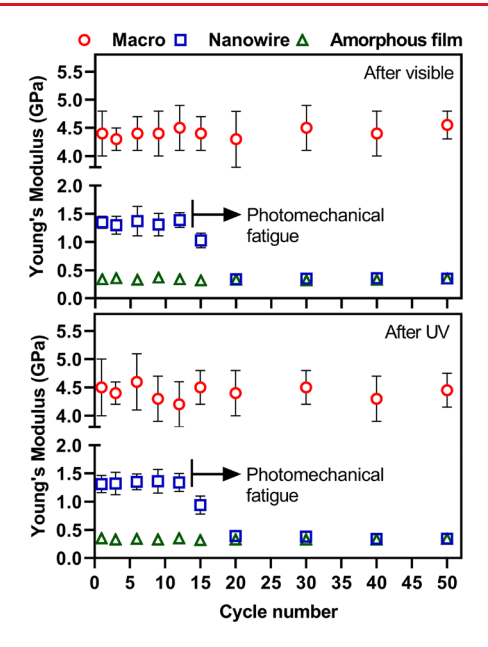


Figure 3. Young's modulus as a function of an increasing number of visible and UV light exposure cycles for a DAE macrocrystal (red circles), nanowire (blue squares), and amorphous film (green triangles). For both macrocrystal and amorphous film samples, the Young's moduli do not change over 50 light exposure cycles. The nanowire sample shows evidence of photomechanical fatigue where Young's modulus starts to decrease after 12 cycles and becomes equal to the Young's modulus of the amorphous film after 20 cycles. Subsequent light exposures up to 50 cycles do not change the nanowire elastic modulus.

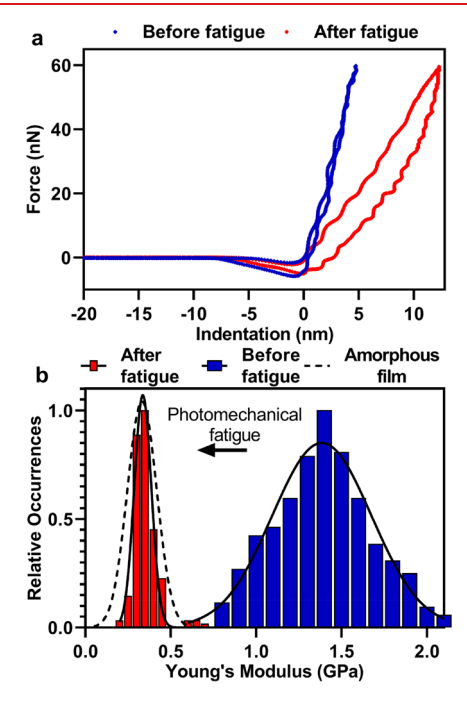


Figure 4. (a) Representative force curves (both approach and retract) collected on DAE nanowire before (blue) and after (red) photomechanical fatigue showing appearance of the hysteresis between the approach and retract data. (b) Histograms of Young's moduli for the DAE nanowire before (blue) and after (red) photomechanical fatigue. Solid black lines are Gaussian fits. The dashed black line is the Gaussian fit for Young's modulus data of amorphous film.

in Figure 4b. Specifically, the fatigue results in 4-fold reduction of the nanowire Young's modulus (1.4 \pm 0.3 GPa to 0.34 \pm 0.05 GPa) and overlaps with the elastic response of the amorphous film (0.35 \pm 0.09 GPa). Additionally, the full width at half-maximum (fwhm) of the nanowire Young's moduli distribution after the fatigue decreases from 0.7 to 0.1 GPa, which is comparable to the fwhm of 0.2 GPa for the amorphous film. The significantly narrower distributions of elastic moduli for the fatigued nanowire and amorphous film are consistent with more homogeneous mechanical response expected for an amorphous solid. 49

Because the fatigued nanowire and amorphous film both exhibit similar Young's modulus values with comparable distributions and similar viscoelastic hysteresis, we attribute the underlying mechanism of the photomechanical fatigue to a physical transformation from the crystalline to amorphous state. To further validate this hypothesis, PXRD data were collected for nanowires laying horizontally on AAO template before and after 10 cycles of visible and UV light exposure (Figure 5). A clear decrease (about 90%) in the peak

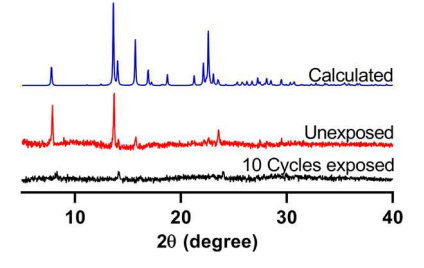


Figure 5. Comparison of DAE nanowires PXRD patterns: simulated pattern (blue), nanowires prior to light exposure (red), and nanowires after 10 cycles of light exposure (black). Significant decrease in the peak intensities as a result of light exposures supports crystalline to amorphous transformation as a result of photomechanical fatigue.

intensities is evident after the repeated light exposures, consistent with our hypothesis for the loss of nanowire crystallinity due to a crystalline to amorphous physical transformation. We note the relatively weak PXRD data are due to the small depth of the nanowire sample needed to ensure sufficient UV light penetration into the solid to maximize conversion efficiency from 1a to 1b.

Dong et al. previously reported that DAE nanowires embedded into an AAO template displayed a steady decrease in photoactuated displacement.²⁵ They attributed this photomechanical fatigue to a chemical reaction between DAE nanowires and AAO template walls.²⁵ Although the DAE derivative used in our experiments has additional methyl groups on the thiophene rings, its photochemistry is expected to be very similar. Our AFM results on isolated nanowires strongly suggest that photomechanical fatigue can result from changes in crystallinity during multiple repeated photoisomerizations. One possible mechanism for the photomechanical fatigue is that an increasing number of surface defects can nucleate and facilitate a crystalline to amorphous transformation. Alternatively, it is possible that chemical side products can also act as defects that nucleate this transition with the nanowires being much more susceptible. While the exact mechanism remains to be confirmed, this study provides first experimental evidence that photomechanical fatigue can be dramatically accelerated in nanocrystals due to a crystalline to amorphous physical transformation. This result suggests that

the intrinsic mechanical properties of bulk macrocrystals may not provide a valid foundation for the design of ultrasmall photomechanical crystals or composites, since both the static (Young's modulus) and dynamic (fatigue resistance) mechanical properties can be very different for nanoscale crystals.

CONCLUSION

In summary, AFM nanoindentation was utilized to quantify changes in elastic modulus (Young's modulus) of single macrocrystals, single crystal nanowires, and amorphous films composed of photochromic DAE molecules. The mechanical properties depend on crystal morphology with DAE nanowire crystals displaying a 3-fold decrease in the Young's modulus compared to macrocrystals. Furthermore, while the Young's modulus values for macrocrystals and amorphous film remain constant over at least 50 light exposure cycles, the nanowires exhibit a dramatic decrease in the Young's modulus after 10—20 cycles. This accelerated photomechanical fatigue is attributed to a loss in crystallinity of the nanowire.

ASSOCIATED CONTENT

Supporting Information

The Supporting Information is available free of charge at https://pubs.acs.org/doi/10.1021/acs.nanolett.0c02631.

Full experimental details including materials, methods, synthesis, and analysis along with characterization data from atomic force microscopy, optical microscopy and powder X-ray diffraction (PDF)

AUTHOR INFORMATION

Corresponding Authors

Christopher J. Bardeen — Department of Chemistry, University of California Riverside, Riverside, California 92521, United States; orcid.org/0000-0002-5755-9476; Email: christopher.bardeen@ucr.edu

Alexei V. Tivanski — Department of Chemistry, The University of Iowa, Iowa City, Iowa 52242, United States; o orcid.org/0000-0002-1528-2421; Email: alexei-tivanski@uiowa.edu

Authors

Thiranjeewa I. Lansakara — Department of Chemistry, The University of Iowa, Iowa City, Iowa 52242, United States; orcid.org/0000-0002-9995-882X

Fei Tong — Department of Chemistry, University of California Riverside, Riverside, California 92521, United States; orcid.org/0000-0003-4545-2230

Complete contact information is available at: https://pubs.acs.org/10.1021/acs.nanolett.0c02631

Author Contributions

The manuscript was written through contributions of all authors. All authors have given approval to the final version of the manuscript.

Funding

T.I.L. was partially supported by a University of Iowa Graduate College Summer Fellowship. C.J.B. and F.T. acknowledge financial support from the National Science Foundation Grant DMR-1810514 and by the MURI on Photomechanical Materials Systems (ONR N00014-18-1-2624).

Notes

The authors declare no competing financial interest.

ABBREVIATIONS

AFM, atomic force microscopy; PXRD, powder X-ray diffraction

REFERENCES

- (1) Kitagawa, D.; Kobatake, S. Crystal Thickness Dependence of Photoinduced Crystal Bending of 1,2-Bis(2-methyl-5-(4-(1-naphthoyloxymethyl)phenyl)-3-thienyl)perfluorocyclopentene. *J. Phys. Chem. C* 2013, *117* (40), 20887–20892.
- (2) Nath, N. K.; Pejov, L.; Nichols, S. M.; Hu, C. H.; Saleh, N.; Kahr, B.; Naumov, P. Model for Photoinduced Bending of Slender Molecular Crystals. *J. Am. Chem. Soc.* **2014**, *136* (7), 2757–2766.
- (3) Koshima, H.; Ojima, N.; Uchimoto, H. Mechanical Motion of Azobenzene Crystals upon Photoirradiation. *J. Am. Chem. Soc.* **2009**, 131 (20), 6890–6891.
- (4) Kitagawa, D.; Nishi, H.; Kobatake, S. Photoinduced Twisting of a Photochromic Diarylethene Crystal. *Angew. Chem., Int. Ed.* **2013**, 52 (35), 9320–9322.
- (5) Al-Kaysi, R. O.; Muller, A. M.; Bardeen, C. J. Photochemically driven shape changes of crystalline organic nanorods. *J. Am. Chem. Soc.* **2006**, *128* (50), 15938–15939.
- (6) Kobatake, S.; Takami, S.; Muto, H.; Ishikawa, T.; Irie, M. Rapid and reversible shape changes of molecular crystals on photo-irradiation. *Nature* **2007**, *446* (7137), 778–781.
- (7) Kitagawa, D.; Okuyama, T.; Tanaka, R.; Kobatake, S. Photoinduced Rapid and Explosive Fragmentation of Diarylethene Crystals Having Urethane Bonding. *Chem. Mater.* **2016**, 28 (14), 4889–4892.
- (8) Wang, H. R.; Chen, P.; Wu, Z.; Zhao, J. Y.; Sun, J. B.; Lu, R. Bending, Curling, Rolling, and Salient Behavior of Molecular Crystals Driven by [2 + 2] Cycloaddition of a Styrylbenzoxazole Derivative. *Angew. Chem., Int. Ed.* **2017**, *56* (32), 9463–9467.
- (9) Bushuyev, O. S.; Singleton, T. A.; Barrett, C. J. Fast, Reversible, and General Photomechanical Motion in Single Crystals of Various Azo Compounds Using Visible Light. *Adv. Mater.* **2013**, 25 (12), 1796–1800.
- (10) Bushuyev, O. S.; Tomberg, A.; Friscic, T.; Barrett, C. J. Shaping Crystals with Light: Crystal-to-Crystal Isomerization and Photomechanical Effect in Fluorinated Azobenzenes. *J. Am. Chem. Soc.* **2013**, 135 (34), 12556–12559.
- (11) Naumov, P.; Kowalik, J.; Solntsev, K. M.; Baldridge, A.; Moon, J. S.; Kranz, C.; Tolbert, L. M. Topochemistry and Photomechanical Effects in Crystals of Green Fluorescent Protein-like Chromophores: Effects of Hydrogen Bonding and Crystal Packing. *J. Am. Chem. Soc.* **2010**, *132* (16), 5845–5857.
- (12) Zhu, L. Y.; Al-Kaysi, R. O.; Bardeen, C. J. Reversible Photoinduced Twisting of Molecular Crystal Microribbons. *J. Am. Chem. Soc.* **2011**, 133 (32), 12569–12575.
- (13) Naumov, P.; Sahoo, S. C.; Zakharov, B. A.; Boldyreva, E. V. Dynamic Single Crystals: Kinematic Analysis of Photoinduced Crystal Jumping (The Photosalient Effect). *Angew. Chem., Int. Ed.* **2013**, *52* (38), 9990–9995.
- (14) Kitagawa, D.; Kobatake, S. Photoreversible current ON/OFF switching by the photoinduced bending of gold-coated diarylethene crystals. *Chem. Commun.* **2015**, *51* (21), 4421–4424.
- (15) Kitagawa, D.; Tanaka, R.; Kobatake, S. Photoinduced stepwise bending behavior of photochromic diarylethene crystals. *CrystEng-Comm* **2016**, *18* (38), 7236–7240.
- (16) Hirano, A.; Hashimoto, T.; Kitagawa, D.; Kono, K.; Kobatake, S. Dependence of Photoinduced Bending Behavior of Diarylethene Crystals on Ultraviolet Irradiation Power. *Cryst. Growth Des.* **2017**, *17* (9), 4819–4825.
- (17) Irie, M.; Fukaminato, T.; Matsuda, K.; Kobatake, S. Photochromism of Diarylethene Molecules and Crystals: Memories, Switches, and Actuators. *Chem. Rev.* **2014**, *114* (24), 12174–12277.
- (18) Irie, M. Diarylethenes for memories and switches. *Chem. Rev.* **2000**, *100* (5), 1685–1716.

- (19) Patel, P. D.; Mikhailov, I. A.; Belfield, K. D.; Masunov, A. E. Theoretical Study of Photochromic Compounds, Part 2: Thermal Mechanism for Byproduct Formation and Fatigue Resistance of Diarylethenes Used as Data Storage Materials. *Int. J. Quantum Chem.* **2009**, *109* (15), 3711–3722.
- (20) Herder, M.; Schmidt, B. M.; Grubert, L.; Patzel, M.; Schwarz, J.; Hecht, S. Improving the Fatigue Resistance of Diarylethene Switches. *J. Am. Chem. Soc.* **2015**, *137* (7), 2738–2747.
- (21) Irie, M.; Lifka, T.; Uchida, K.; Kobatake, S.; Shindo, Y. Fatigue resistant properties of photochromic dithienylethenes: by-product formation. *Chem. Commun.* **1999**, No. 8, 747–748.
- (22) Terao, F.; Morimoto, M.; Irie, M. Light-Driven Molecular-Crystal Actuators: Rapid and Reversible Bending of Rodlike Mixed Crystals of Diarylethene Derivatives. *Angew. Chem., Int. Ed.* **2012**, *51* (4), 901–904.
- (23) Tong, F.; Kitagawa, D.; Dong, X. N.; Kobatake, S.; Bardeen, C. J. Photomechanical motion of diarylethene molecular crystal nanowires. *Nanoscale* **2018**, *10* (7), 3393–3398.
- (24) Fu, Q. T.; Yan, X. D.; Li, T.; Zhang, X. Y.; He, Y.; Zhang, W. D.; Liu, Y.; Li, Y. X.; Gu, Z. G. Diarylethene-based conjugated polymer networks for ultrafast photochromic films. *New J. Chem.* **2019**, 43 (39), 15797–15803.
- (25) Dong, X. M.; Tong, F.; Hanson, K. M.; Al-Kaysi, R. O.; Kitagawa, D.; Kobatake, S.; Bardeen, C. J. Hybrid Organic Inorganic Photon-Powered Actuators Based on Aligned Diarylethene Nanocrystals. *Chem. Mater.* **2019**, *31* (3), 1016–1022.
- (26) Tong, F.; Liu, M. Y.; Al-Kaysi, R. O.; Bardeen, C. J. Surfactant-Enhanced Photoisomerization and Photomechanical Response in Molecular Crystal Nanowires. *Langmuir* **2018**, 34 (4), 1627–1634.
- (27) Naumov, P.; Chizhik, S.; Panda, M. K.; Nath, N. K.; Boldyreva, E. Mechanically Responsive Molecular Crystals. *Chem. Rev.* **2015**, *115* (22), 12440–12490.
- (28) Rupasinghe, T. P.; Hutchins, K. M.; Bandaranayake, B. S.; Ghorai, S.; Karunatilake, C.; Bucar, D. K.; Swenson, D. C.; Arnold, M. A.; MacGillivray, L. R.; Tivanski, A. V. Mechanical Properties of a Series of Macro- and Nanodimensional Organic Cocrystals Correlate with Atomic Polarizability. *J. Am. Chem. Soc.* **2015**, *137* (40), 12768–12771.
- (29) Karunatilaka, C.; Bucar, D. K.; Ditzler, L. R.; Friscic, T.; Swenson, D. C.; MacGillivray, L. R.; Tivanski, A. V. Softening and Hardening of Macro- and Nano-Sized Organic Cocrystals in a Single-Crystal Transformation. *Angew. Chem., Int. Ed.* **2011**, *50* (37), 8642–8646.
- (30) Hutchins, K. M.; Rupasinghe, T. P.; Ditzler, L. R.; Swenson, D. C.; Sander, J. R. G.; Baltrusaitis, J.; Tivanski, A. V.; MacGillivray, L. R. Nanocrystals of a Metal-Organic Complex Exhibit Remarkably High Conductivity that Increases in a Single-Crystal-to-Single-Crystal Transformation. J. Am. Chem. Soc. 2014, 136 (19), 6778–6781.
- (31) Root, S. E.; Savagatrup, S.; Printz, A. D.; Rodriquez, D.; Lipomi, D. J. Mechanical Properties of Organic Semiconductors for Stretchable, Highly Flexible, and Mechanically Robust Electronics. *Chem. Rev.* **2017**, *117* (9), 6467–6499.
- (32) Chibani, S.; Coudert, F. X. Systematic exploration of the mechanical properties of 13 621 inorganic compounds. *Chemical Science* **2019**, *10* (37), 8589–8599.
- (33) Zhu, L. Y.; Tong, F.; Salinas, C.; Al-Muhanna, M. K.; Tham, F. S.; Kisailus, D.; Al-Kaysi, R. O.; Bardeen, C. J. Improved Solid-State Photomechanical Materials by Fluorine Substitution of 9-Anthracene Carboxylic Acid. *Chem. Mater.* **2014**, *26* (20), 6007–6015.
- (34) Almadori, Y.; Moerman, D.; Martinez, J. L.; Leclere, P.; Grevin, B. Multimodal noncontact atomic force microscopy and Kelvin probe force microscopy investigations of organolead tribromide perovskite single crystals. *Beilstein J. Nanotechnol.* **2018**, *9*, 1695–1704.
- (35) Yamada, T.; Muto, K.; Kobatake, S.; Irie, M. Crystal structure-reactivity correlation in single-crystalline photochromism of 1,2-bis(2-methyl-5-phenyl-3-thienyl)perfluorocyclopentene. *J. Org. Chem.* **2001**, 66 (18), 6164–6168.

- (36) Tsujioka, T.; Kume, M.; Irie, M. Photochromic reactions of a diarylethene derivative in polymer matrices. *J. Photochem. Photobiol., A* **1997**, *104* (1–3), 203–206.
- (37) Kim, M.; Yun, J. H.; Cho, M. Light penetration-coupled photoisomerization modeling for photodeformation of diarylethene single crystal: upscaling isomerization to macroscopic deformation. *Sci. Rep.* **2017**, *7*, 967.
- (38) Sumi, T.; Takagi, Y.; Yagi, A.; Morimoto, M.; Irie, M. Photoirradiation wavelength dependence of cycloreversion quantum yields of diarylethenes. *Chem. Commun.* **2014**, *S0* (30), 3928–3930.
- (39) Jee, A. Y.; Lee, M. Comparative analysis on the nano-indentation of polymers using atomic force microscopy. *Polym. Test.* **2010**, 29 (1), 95–99.
- (40) Hutchins, K. M.; Rupasinghe, T. P.; Oburn, S. M.; Ray, K. K.; Tivanski, A. V.; MacGillivray, L. R. Remarkable decrease in stiffness of aspirin crystals upon reducing crystal size to nanoscale dimensions via sonochemistry. *CrystEngComm* **2019**, 21 (13), 2049–2052.
- (41) Ohshima, S.; Morimoto, M.; Irie, M. Light-driven bending of diarylethene mixed crystals. *Chem. Sci.* **2015**, 6 (10), 5746–5752.
- (42) Tiba, A.; Tivanski, A. V.; MacGillivray, L. R. Size-Dependent Mechanical Properties of a Metal-Organic Framework: Increase in Flexibility of ZIF-8 by Crystal Downsizing. *Nano Lett.* **2019**, *19* (9), 6140–6143.
- (43) Huxter, V. M.; Lee, A.; Lo, S. S.; Scholes, G. D. CdSe Nanoparticle Elasticity and Surface Energy. *Nano Lett.* **2009**, 9 (1), 405–409.
- (44) Xu, W. W.; Davila, L. P. Size dependence of elastic mechanical properties of nanocrystalline aluminum. *Mater. Sci. Eng., A* **2017**, *692*, 90–94.
- (45) Morimoto, M.; Irie, M. A Diarylethene Cocrystal that Converts Light into Mechanical Work. *J. Am. Chem. Soc.* **2010**, *132* (40), 14172–14178.
- (46) Ray, K. K.; Lee, H. D.; Gutierrez, M. A.; Chang, F. J.; Tivanski, A. V. Correlating 3D Morphology, Phase State, and Viscoelastic Properties of Individual Substrate-Deposited Particles. *Anal. Chem.* **2019**, *91* (12), 7621–7630.
- (47) Lee, H. D.; Ray, K. K.; Tivanski, A. V. Solid, Semisolid, and Liquid Phase States of Individual Submicrometer Particles Directly Probed Using Atomic Force Microscopy. *Anal. Chem.* **2017**, 89 (23), 12720–12726.
- (48) Bremmell, K. E.; Evans, A.; Prestidge, C. A. Deformation and nano-rheology of red blood cells: An AFM investigation. *Colloids Surf., B* **2006**, *50* (1), 43–48.
- (49) Ward, S.; Perkins, M.; Zhang, J. X.; Roberts, C. J.; Madden, C. E.; Luk, S. Y.; Patel, N.; Ebbens, S. J. Identifying and mapping surface amorphous domains. *Pharm. Res.* **2005**, 22 (7), 1195–1202.